

## Theory of scattering between two phonon beams in superfluid helium

I. N. Adamenko,<sup>1</sup> Yu. A. Kitsenko,<sup>2</sup> K. E. Nemchenko,<sup>1</sup> and A. F. G. Wyatt<sup>3,\*</sup>

<sup>1</sup>Karazin Kharkov National University, Svobody Sq. 4, Kharkov 61077, Ukraine

<sup>2</sup>Akhiezer Institute for Theoretical Physics, National Science Center Kharkov Institute of Physics and Technology, National Academy of Sciences of Ukraine, 1 Akademicheskaya St., Kharkov 61108, Ukraine

<sup>3</sup>School of Physics, University of Exeter, Exeter EX4 4QL, United Kingdom

(Received 13 February 2009; published 13 July 2009)

We calculate the interactions between pairs of phonon beams in liquid  $^4\text{He}$ , in particular  $l$ - $l$ ,  $h$ - $l$ , and  $h$ - $h$  beams, where  $l$  and  $h$  stand for low- and high-energy phonons, respectively. This entails calculating the rate of four-phonon process (4pp) scattering for the whole phonon momentum range in liquid helium taking into account the momentum distribution of the phonons in the beams. The attenuation coefficient of one beam due to the other is calculated for each case, and the results are compared with experimental data. We find broad quantitative agreement that confirms the 4pp scattering theory.

DOI: [10.1103/PhysRevB.80.014509](https://doi.org/10.1103/PhysRevB.80.014509)

PACS number(s): 67.25.-k

### I. INTRODUCTION

Most of the properties of liquid  $^4\text{He}$  can be understood within the excitation picture introduced by Landau<sup>1</sup> (see also Ref. 2). In this model, the liquid helium is considered to be excitations from a ground state, which acts as a “vacuum” state for the excitations. The excitations are phonons and rotons and, as they are long-lived excitations, they can be treated as quasiparticles that move through the vacuum state. This model gives a good description of the thermodynamic properties of liquid helium, such as the heat capacity. Also, as the excitations are identified with the normal fluid, it also explains the underlying basis for the two-fluid model,<sup>1,3</sup> which so well describes the hydrodynamics of superfluid helium.

However there are interactions between the quasiparticles, so they scatter each other, and this gives the quasiparticles a finite lifetime. This lifetime usually, but not always,<sup>4</sup> depends on the ambient density of the quasiparticles. The roton lifetime can be directly seen in neutron-scattering experiments as a broadening of the linewidth with increasing temperature.<sup>5,6</sup> The quasiparticle scattering also explains such bulk properties as the normal fluid viscosity<sup>7,8</sup> and sound attenuation.<sup>9</sup>

Theories of scattering were initially applied to explain these bulk properties, which meant considering the interaction of a typical quasiparticle with an isotropic distribution of quasiparticles in thermodynamic equilibrium. It was the failure to explain sound attenuation that led to the suggestion that the dispersion curve was not linear at low momenta but that phonon energy increased faster than linearly with momentum.<sup>9</sup>

The theory of interactions between phonons showed that the scattering is strongly dependent on the angle between the two incoming quasiparticles, as well as on their momenta. So when phonon-phonon interactions are evaluated in isotropic liquid helium, all the details of the angular dependence are lost in the averaging over all angles. This means that the theories of scattering are not confirmed in detail.

In order to test the theories of phonon-phonon interaction, one would need to create a beam of well-defined phonons

and measure their interaction with a second beam of well-defined phonons, in much the same way that high-energy particle experiments are conducted. However the phonons in a beam may or may not be interacting, so the situation may not be as simple as considering beams of independent particles. The parameters of a phonon beam change with time as the beam propagates in the superfluid helium. If the interactions between the phonons, within a beam, are so strong that the relaxation time of phonons is much smaller than the typical time of variation of the parameters in the beam, then these phonons can be described by a local equilibrium distribution function in space and time. This function describes an anisotropic phonon system, and it will be essentially different to that for the isotropic distribution. It turns out that one can still have a beam with reasonably well-defined narrow angle, even when the phonons in the beam are interacting rapidly. A calculation of the scattering between two beams must take into account the spectrum of phonon energies in the beams as well as the angle between the beams.

Recently measurements of the scattering between beams of different phonons had been published.<sup>10</sup> The experiments considered three different types of scattering, (i) scattering between two beams of low-energy phonons, (ii) scattering between low-energy and high-energy phonons, and (iii) scattering between two beams of high-energy phonons. These will be referred to as  $l$ - $l$ ,  $h$ - $l$ , and  $h$ - $h$  scatterings, respectively. Interactions between these two groups of phonons is a natural choice as groups of low- and high-energy phonons form in the liquid  $^4\text{He}$  due to the shape of the dispersion curve.<sup>11-13</sup> Low-energy phonons ( $l$  phonons) are defined by their momentum  $p$  being less than  $p_c$ , and high-energy phonons ( $h$  phonons) are defined by  $p > p_c$ , where  $p_c$  is the momentum where  $cp_c = \varepsilon$ , where  $c$  is the velocity of sound as  $p \rightarrow 0$  and  $\varepsilon$  is the phonon energy. At saturated vapor pressure, at  $T < 1$  K,  $\tilde{p}_c = cp_c/k_B = 10$  K.

The experimental technique of Ref. 10 allows two phonon beams to scatter at different angles to each other. These different angles, between the phonon beams in experiment, were realized by using different groups of heaters. The bolometer was positioned in front of one of the two heaters, and this defined the probe beam. In the set of experiments,

phonon beams scattered at three different angles: 30, 40, and 160°.

These measurements have stimulated the need to create a quantitative theory to compare with them, and this we present here. We shall see that there is satisfactory agreement between the experiment and the theory, which gives confidence that the description of the interaction between phonons of superfluid helium—based on quantized hydrodynamic Landau Hamiltonian—works well.<sup>1</sup>

In this paper we shall be concerned with scattering by four-phonon processes (4pps). We will discuss the interaction between  $l$ -phonon beams that are at large angle to each other and also between two beams, one of which is an  $h$ -phonon beam. In both cases three-phonon processes (3pps) are forbidden by the conservation laws of energy and momentum. When the angle between the phonons is small, certainly less than 27° and usually smaller depending on the phonon energies, and the phonon energies are less than 10 K, then 3pps are allowed. Usually the 3pp scattering rate is so high that the attenuation of one  $l$ -phonon beam by another  $l$ -phonon beam is too high to measure.

Historically only 4pp interactions were thought to be significant in liquid <sup>4</sup>He because the phonon dispersion curve was thought to deviate downwards from linearity. However after it was suggested<sup>9</sup> and then confirmed<sup>14,15</sup> that the dispersion curve initially increased faster than linearly, then 3pp scattering was analyzed and found to be important.<sup>16–18</sup> Scattering by 3pp leads to both spontaneous decay of low-energy phonons and to strong interactions between two low-energy phonons if the angle between them is small. As 3pp scattering does not conserve the number of phonons, it is this process that allows thermal equilibrium to be attained. For large angles, 3pp scattering is forbidden by conservation laws of energy and momentum and then 4pp is the dominant scattering process.

The first analysis of 4pp interactions was by Landau and Khalatnikov<sup>7</sup> (see also Ref. 2) using a quantized hydrodynamic model. All Landau and Khalatnikov calculations were made on the assumption that in superfluid helium the dispersion curve is normal; i.e., it bends downwards from a linear law. For anomalous dispersion, i.e., the dispersion curve bending upwards from linearity, the results of Landau and Khalatnikov<sup>7</sup> are not applicable. The first good calculation of 4pp scattering was by Tucker and Wyatt,<sup>19</sup> and this gave agreement with measurements.

In the momentum and angular ranges where 3pps are allowed, we have recently shown that 4pp scattering rates are almost exactly equivalent to the 3pp rates.<sup>8</sup> The matrix element for 4pp, in second-order perturbation theory of small deviations of the system from equilibrium, diverges when there is faster than linear dispersion, so the analysis had to overcome this problem. The 4pp rate is almost the same as the 3pp rate in these ranges because two successive 3pp scatterings look like one 4pp scattering. This is an important result as it points to the error in counting both the 3pp and 4pp contributions to the scattering rate. All 4pps that can be rewritten as two 3pp scatterings should be ignored in calculating the total scattering rate by summing 3pp and 4pp rates.

In order to calculate the interaction rate between two phonon beams, it is necessary to model the momentum spectrum

in the beams as well as to calculate the matrix elements. This is done using the anisotropic phonon distribution that was introduced in Ref. 20. In previous work we have used an approximate distribution function, the Bose-cone approximation. So in the sections of previous papers, for example,<sup>21</sup> where the approximate distribution function was used, the present work supersedes the earlier work.

In Sec. II we give the details of the derivation of the 4pp scattering matrix elements. In Secs. III–V we consider  $l$ - $l$ ,  $h$ - $l$ , and  $h$ - $h$  phonon scattering, respectively. Finally in Sec. VI we draw our conclusions. We give the relationships between the angles for the matrix element in the Appendix.

## II. FOUR-PHONON SCATTERING RATES, INCLUDING THE MOMENTUM RANGE WHERE THREE-PHONON PROCESSES ARE POSSIBLE

We consider four-phonon process in which there are two phonons in the initial state and two phonons in the final state. The conservation of energy and momentum gives

$$\varepsilon_1 + \varepsilon_2 = \varepsilon_3 + \varepsilon_4, \quad \mathbf{p}_1 + \mathbf{p}_2 = \mathbf{p}_3 + \mathbf{p}_4. \quad (1)$$

The kinetic equation describing the change in the distribution function  $n(\mathbf{p}_1) \equiv n_1$ , due to process (1), can be written as

$$\frac{dn_1}{dt} = N_b(\mathbf{p}_1) - N_d(\mathbf{p}_1). \quad (2)$$

Here  $N_b(\mathbf{p}_1)$  and  $N_d(\mathbf{p}_1)$  are the rates of increasing and decreasing numbers of phonons with momentum  $\mathbf{p}_1$  in unit time due to collisions, respectively. They can be written as

$$N_{b,d}(\mathbf{p}_1) = \int W(\mathbf{p}_1, \mathbf{p}_2 | \mathbf{p}_3, \mathbf{p}_4) \delta(\mathbf{p}_\Sigma) \delta(\varepsilon_\Sigma) n_{b,d} d^3 p_2 d^3 p_3 d^3 p_4. \quad (3)$$

Here  $W(\mathbf{p}_1, \mathbf{p}_2 | \mathbf{p}_3, \mathbf{p}_4)$  is the probability density for process (1), the  $\delta$  functions correspond to the conservation laws of energy  $\varepsilon_\Sigma = \varepsilon_1 + \varepsilon_2 - \varepsilon_3 - \varepsilon_4$  and momentum  $\mathbf{p}_\Sigma = \mathbf{p}_1 + \mathbf{p}_2 - \mathbf{p}_3 - \mathbf{p}_4$  and

$$n_b = n_3 n_4 (1 + n_2) (1 + n_1), \quad n_d = n_1 n_2 (1 + n_3) (1 + n_4). \quad (4)$$

Equation (3) is integrated over  $p_3$  and  $p_4$ , with the condition that  $p_3 > p_4$  to avoid double counting. The distribution functions that enter into Eq. (3) are determined by particular problem under consideration. Thus, in case of  $l$ -phonon pulse, in which the equilibrium due to three-phonon processes with typical time  $\tau_{3pp}$  is quickly attained in comparison with all other times of the system  $\tau_r$ , in the zeroth approximation of small parameter  $\tau_{3pp} / \tau_r \ll 1$  the local-equilibrium Bose distribution can be taken as the distribution function of  $l$ -phonon system. For this the phonon system must be rather dilute so that the energy uncertainty, due to the interaction of phonons, should be much smaller than the phonon energy  $\varepsilon(p)$ . So the method, which is here developed, can be used when

$$\hbar/\varepsilon(p) \ll \tau_{3pp} \ll \tau_t. \quad (5)$$

We note that in our system this inequality is always satisfied as our typical times are equal to  $\tau_{3pp} \sim 10^{-9}$  s,<sup>18</sup>  $\tau_t \sim 10^{-5}$  s,<sup>22</sup> and  $\hbar/\varepsilon(p) \sim 10^{-12}$  s for thermal phonons.

Using Eq. (3), the relation for  $N_d$  can be written as

$$N_d = n_1 \nu_d, \quad (6)$$

where

$$\nu_d(\mathbf{p}_1) = \int d^3 p_2 d^3 p_3 d^3 p_4 W(\mathbf{p}_1, \mathbf{p}_2 | \mathbf{p}_3, \mathbf{p}_4) \delta(\mathbf{p}_\Sigma) \delta(\varepsilon_\Sigma) n_2(1 + n_3)(1 + n_4). \quad (7)$$

The rate  $\nu_d(\mathbf{p}_1)$  determines the relaxation time in the phonon system, when  $N_b=0$ , i.e., when the creation rate of  $p_1$  is zero.

To obtain the rate  $\nu_d$  we must find the probability density of four-phonon processes  $W(\mathbf{p}_1, \mathbf{p}_2 | \mathbf{p}_3, \mathbf{p}_4)$ , which enters into Eq. (7). The interaction of phonons in superfluid helium can be described by the Landau Hamiltonian, which can be written as (see, for example, Ref. 2)

$$\hat{H}_{ph} = \hat{H}_0 + \hat{V}_3 + \hat{V}_4. \quad (8)$$

Here  $\hat{H}_0$  is the Hamiltonian of noninteracting phonons, and terms  $\hat{V}_3$  and  $\hat{V}_4$  describe the interaction of phonons caused by the third and fourth orders of small deviations of the system, from an equilibrium state of helium, respectively.

In second quantization the operator for three-particle interactions  $\hat{V}_3$  can be written as (for details see Refs. 2, 17, and 18)

$$\hat{V}_3 = \frac{1}{6c} \frac{1}{\sqrt{8\rho V}} \sum_{\mathbf{p}_\alpha, \mathbf{p}_\beta, \mathbf{p}_\gamma} \delta_{\mathbf{p}_\alpha + \mathbf{p}_\beta + \mathbf{p}_\gamma, 0} \sqrt{\varepsilon_\alpha \varepsilon_\beta \varepsilon_\gamma} \{ (2u-1)(\hat{a}_{\mathbf{p}_\alpha} + \hat{a}_{-\mathbf{p}_\alpha}^+)(\hat{a}_{\mathbf{p}_\beta} + \hat{a}_{-\mathbf{p}_\beta}^+)(\hat{a}_{\mathbf{p}_\gamma} + \hat{a}_{-\mathbf{p}_\gamma}^+) + 3\mathbf{n}_\alpha \mathbf{n}_\gamma (\hat{a}_{\mathbf{p}_\alpha} - \hat{a}_{-\mathbf{p}_\alpha}^+)(\hat{a}_{\mathbf{p}_\beta} + \hat{a}_{-\mathbf{p}_\beta}^+)(\hat{a}_{\mathbf{p}_\gamma} - \hat{a}_{-\mathbf{p}_\gamma}^+) \}, \quad (9)$$

and for four-particle interactions  $\hat{V}_4$  we have

$$\hat{V}_4 = \frac{(u-1)^2 + w}{48\rho V c^2} \sum_{\mathbf{p}_\alpha, \mathbf{p}_\beta, \mathbf{p}_\gamma, \mathbf{p}_\delta} \delta_{\mathbf{p}_\alpha + \mathbf{p}_\beta + \mathbf{p}_\gamma + \mathbf{p}_\delta, 0} \sqrt{\varepsilon_\alpha \varepsilon_\beta \varepsilon_\gamma \varepsilon_\delta} (\hat{a}_{\mathbf{p}_\alpha} + \hat{a}_{-\mathbf{p}_\alpha}^+)(\hat{a}_{\mathbf{p}_\beta} + \hat{a}_{-\mathbf{p}_\beta}^+)(\hat{a}_{\mathbf{p}_\gamma} + \hat{a}_{-\mathbf{p}_\gamma}^+)(\hat{a}_{\mathbf{p}_\delta} + \hat{a}_{-\mathbf{p}_\delta}^+). \quad (10)$$

Here  $\hat{a}_{\mathbf{p}}^+$  and  $\hat{a}_{\mathbf{p}}$  are the creation and annihilation operators, respectively, for a phonon with momentum  $\mathbf{p}$ ,  $\mathbf{n}_i = \frac{\mathbf{p}_i}{p_i}$ ,  $\varepsilon_i = \varepsilon(\mathbf{p}_i)$ ,  $u = \frac{\rho}{c} \frac{\partial c}{\partial \rho} = 2.84$  is the Grüneisen constant,  $w = \frac{\rho^2}{c} \frac{\partial^2 c}{\partial \rho^2} = 0.188$ ,  $V$  is the volume of the system, and  $\rho = 145$  kg/m<sup>3</sup> is the density of He II.

The probability density, for the four-phonon process, can be written as Refs. 19 and 21–23,

$$W(\mathbf{p}_1, \mathbf{p}_2 | \mathbf{p}_3, \mathbf{p}_4) = \frac{2\pi}{\hbar} V^2 |H_{fi}|^2 \frac{1}{(2\pi\hbar)^6}. \quad (11)$$

Here  $H_{fi}$  is the amplitude of the four-phonon process obtained in second-order perturbation theory with  $\hat{V}_3$  and in first-order perturbation theory with  $\hat{V}_4$  in the standard way (see for example Refs. 23–25) according to which

$$H_{fi} = \sum_{\mathbf{Q}} \frac{\langle \mathbf{p}_3, \mathbf{p}_4 | \hat{V}_3 | \mathbf{Q} \rangle \langle \mathbf{Q} | \hat{V}_3 | \mathbf{p}_1, \mathbf{p}_2 \rangle}{E_i - E_{\mathbf{Q}}} + \langle \mathbf{p}_3, \mathbf{p}_4 | \hat{V}_4 | \mathbf{p}_1, \mathbf{p}_2 \rangle. \quad (12)$$

Here  $E_i$  is the energy of the initial state and  $|\mathbf{Q}\rangle$  is the intermediate state with energy  $E_{\mathbf{Q}}$ .

There are six possible intermediate states  $|\mathbf{Q}\rangle$  from Eq. (9),

$$\text{I. } |\mathbf{p}_1 + \mathbf{p}_2\rangle,$$

$$\text{II. } |\mathbf{p}_2, \mathbf{p}_3, \mathbf{p}_1 - \mathbf{p}_3\rangle,$$

$$\text{III. } |\mathbf{p}_2, \mathbf{p}_4, \mathbf{p}_1 - \mathbf{p}_4\rangle,$$

$$\text{IV. } |\mathbf{p}_1, \mathbf{p}_3, \mathbf{p}_2 - \mathbf{p}_3\rangle,$$

$$\text{V. } |\mathbf{p}_1, \mathbf{p}_4, \mathbf{p}_2 - \mathbf{p}_4\rangle,$$

$$\text{VI. } |\mathbf{p}_1, \mathbf{p}_2, \mathbf{p}_3, \mathbf{p}_4, -\mathbf{p}_1 - \mathbf{p}_2\rangle. \quad (13)$$

If all four phonons participating in four-phonon process are  $l$  phonons then it is possible that for some value of  $\mathbf{Q}$ ,  $E_i - E_{\mathbf{Q}} = 0$  and then matrix element, in Eq. (12), diverges. This happens when the transition from the initial state to the final state can be realized by two three-phonon processes. In this case the intermediate state  $|\mathbf{Q}\rangle$  is not a virtual state but is a real state. Thus, not only momentum of the states is conserved but the energy is conserved too ( $E_i = E_{\mathbf{Q}}$ ). This leads to the singularity in matrix element (12). In this case the perturbation theory is also applicable, but it should be modified. We note that similar divergences appear and in the other areas of physics. For example in quantum electrodynamics such divergences appear in the problem of resonant fluorescence (see, for example, Ref. 26). To eliminate this diver-

gence, we must take into account that the energy of a state, which can decay, can only be determined to within an accuracy of  $\Gamma = \hbar/\tau$ , where  $\tau$  is a lifetime of the state (see, for example, Ref. 27). In our case the finiteness of the lifetime of the state  $|\mathbf{Q}\rangle$  is due to the possibility of it decaying by 3pp.

Thus we must substitute for  $E_i - E_{\mathbf{Q}}$ , in the denominator of the first term in Eq. (12), the term  $E_i - E_{\mathbf{Q}} + i\Gamma^{(\mathbf{Q})}$ , where  $\Gamma^{(\mathbf{Q})}$  is the energy width of the intermediate state  $|\mathbf{Q}\rangle$  due to it decaying by 3pp. The lifetimes of the various intermediate states are

$$\begin{aligned} \text{I. } \tau_{(1)} &= \nu_d^{-1}(\mathbf{p}_1 + \mathbf{p}_2), \\ \text{II. } \tau_{(13)} &= \nu_c^{-1}(\mathbf{p}_1 - \mathbf{p}_3), \\ \text{III. } \tau_{(14)} &= \nu_c^{-1}(\mathbf{p}_1 - \mathbf{p}_4), \\ \text{IV. } \tau_{(23)} &= \nu_c^{-1}(\mathbf{p}_2 - \mathbf{p}_3), \\ \text{V. } \tau_{(24)} &= \nu_c^{-1}(\mathbf{p}_2 - \mathbf{p}_4), \\ \text{VI. } \tau_{(5)} &= \infty. \end{aligned} \quad (14)$$

Here  $\nu_d(\mathbf{p})$  is the spontaneous rate of a decay of a phonon with momentum  $\mathbf{p}$  into two, and  $\nu_c(\mathbf{p})$  is the rate of combination of a phonon with momentum  $\mathbf{p}$  with another phonon by 3pp scattering. These rates were calculated by us in Ref. 18 for both isotropic and anisotropic phonon systems. For intermediate state VI, the denominator in Eq. (12) never vanishes and so  $\hbar/\tau_5 = 0$ .

From relations (12) and (13) it follows that

$$H_{fi} = \frac{\sqrt{p_1 p_2 p_3 p_4}}{8\rho V} M_{\Sigma}, \quad (15)$$

where

$$M_{\Sigma} = M^{(1)} + M_{13}^{(3)} + M_{14}^{(3)} + M_{23}^{(3)} + M_{24}^{(3)} + M^{(5)} + M_4 \quad (16)$$

is a matrix element that consists of seven terms, six of which correspond to six intermediate states [Eq. (13)] and the seventh is determined by  $\hat{V}_4$  calculated by perturbation theory to first order. We can write these terms as

$$\begin{aligned} M^{(1)} &= \frac{\varepsilon_{1+2}}{\varepsilon_1 + \varepsilon_2 - \varepsilon_{1+2} + i\Gamma^{(1)}} (2u - 1 + \mathbf{n}_1 \mathbf{n}_2 + \mathbf{n}_1 \mathbf{n}_{1+2} + \mathbf{n}_2 \mathbf{n}_{1+2}) \\ &\quad \times (2u - 1 + \mathbf{n}_3 \mathbf{n}_4 + \mathbf{n}_3 \mathbf{n}_{3+4} + \mathbf{n}_4 \mathbf{n}_{3+4}), \end{aligned} \quad (17)$$

$$\begin{aligned} M^{(5)} &= - \frac{\varepsilon_{1+2}}{\varepsilon_1 + \varepsilon_2 + \varepsilon_{1+2}} (2u - 1 + \mathbf{n}_1 \mathbf{n}_2 - \mathbf{n}_1 \mathbf{n}_{1+2} - \mathbf{n}_2 \mathbf{n}_{1+2}) (2u \\ &\quad - 1 + \mathbf{n}_3 \mathbf{n}_4 - \mathbf{n}_3 \mathbf{n}_{3+4} - \mathbf{n}_4 \mathbf{n}_{3+4}), \end{aligned} \quad (18)$$

$$M_4 = 4\{(u-1)^2 + w\}, \quad (19)$$

$$\begin{aligned} M_{13}^{(3)} &= \frac{\varepsilon_{1-3}}{\varepsilon_1 - \varepsilon_3 - \varepsilon_{1-3} + i\Gamma^{(13)}} (2u - 1 + \mathbf{n}_1 \mathbf{n}_3 + \mathbf{n}_1 \mathbf{n}_{1-3} \\ &\quad + \mathbf{n}_3 \mathbf{n}_{1-3}) (2u - 1 + \mathbf{n}_2 \mathbf{n}_4 + \mathbf{n}_2 \mathbf{n}_{1-3} + \mathbf{n}_4 \mathbf{n}_{1-3}), \end{aligned} \quad (20)$$

where  $\Gamma^{(q)} = \hbar\tau_{(q)}^{-1}$ . The rest of the terms in Eq. (16), i.e.,  $M_{14}^{(3)}$ ,  $M_{23}^{(3)}$ , and  $M_{24}^{(3)}$ , can be obtained from  $M_{13}^{(3)}$  by replacing the corresponding subscripts. The matrix elements are given in detail in the Appendix.

### III. *l-l* PHONON SCATTERING

Anisotropic phonon pulses, described by the equilibrium distribution function, have phonons with momenta strongly peaked in the direction of the pulse propagation. Nevertheless there are phonons with momenta in all directions. When two phonon pulses pass through each other at an angle  $\alpha$ , there are always phonons in one pulse that can interact with a phonon in the other pulse. However the scattering rate is proportional to the number of scattering phonons with the correct momentum, and away from the anisotropy axis—which is along the propagation direction—this number can be very small. This means that when  $\alpha$  is greater than  $\approx 40^\circ$  the scattering rate caused by 3pp is very low.

The angular dependence due to 3pp has been analyzed in Refs. 18 and 20. It was shown that when  $\alpha \sim 0$  the interaction is strong. It reaches a peak when  $\alpha \sim 6^\circ$  as at this angle there is the highest number of suitable scattering phonons. At larger angles the scattering decreases due to the decreasing number of scattering phonons with suitable momentum. At angles  $\alpha \sim 40^\circ$  the interaction between the pulses is very weak. This is similar to that found experimentally.<sup>10</sup> However, phonons in the two pulses can also interact by 4pp, and in this section we analyze 4pp scattering between *l* phonons.

The general problem of the interaction of two phonon pulses is a difficult nonlinear problem. Therefore we restrict ourselves to a solution of the problem of one *l*-phonon scattering with an *l*-phonon pulse. Such scattering can create another *l* phonon or an *h* phonon. These processes can be written as

$$l_1 + l_2 \leftrightarrow l_3 + l_4 \quad (\text{type } ll1),$$

$$l_1 + l_2 \leftrightarrow h_3 + l_4 \quad (\text{type } ll2). \quad (21)$$

We first consider scattering by the first process. The scattering rate can be found from relation (7), but it is more accurately determined from the kinetic equation (2) because this takes into account creation processes as well as decay. Hence in Eq. (2) we assume that

$$n_i = n_i^{(0)} + \delta n_i, \quad n_2 = n_2^{(0)}, \quad n_3 = n_3^{(0)}, \quad n_4 = n_4^{(0)}. \quad (22)$$

In Eq. (22) superscript “0” corresponds to the equilibrium distribution function, and  $\delta n$  is a deviation of the distribution function from equilibrium.

The local-equilibrium distribution function for *l* phonons in a pulse can be written as<sup>18,20</sup>

$$n^{(0)}(\mathbf{p}_l) = \left\{ \exp\left(\frac{\varepsilon_l - \mathbf{p}_l \mathbf{u}}{k_B T}\right) - 1 \right\}^{-1}. \quad (23)$$

Here,

$$\mathbf{u} = \mathbf{N}c(1 - \chi) \quad (24)$$

is a drift velocity,  $\mathbf{N}$  is the unit vector directed along the total momentum of the phonon system, which defines the anisotropy axis of a phonon system, and  $\chi$  is the anisotropy parameter.

In weakly anisotropic systems, the parameter  $\chi$  is close to 1, and when  $\chi=1$  distribution (23) is isotropic. In the systems studied experimentally—see, for example, Refs. 10, 28, and 29—the phonon pulses are strongly anisotropic phonon systems with  $\chi \ll 1$ .

The typical relaxation rate,  $\nu_{ll1}$ , of one  $l$  phonon scattered by a pulse of  $l$  phonons by  $ll1$  processes, in the relaxation time approximation as in kinetic theory, can be written as

$$\nu_{ll1}(\mathbf{p}_1) = -\frac{1}{\delta n_1} \frac{d\delta n_1}{dt}. \quad (25)$$

From Eqs. (2)–(4), (22), and (25) we find that

$$\nu_{ll1}(\mathbf{p}_1) = \frac{1}{1 + n_1^{(0)}} \int_{p_2 \leq p_c} d^3 p_2 \int_{\substack{p_{3low} \leq p_3 \\ p_3 \leq p_{3up}}} d^3 p_3 \int_{p_4 \leq p_3} d^3 p_4 W(\mathbf{p}_1, \mathbf{p}_2 | \mathbf{p}_3, \mathbf{p}_4) \delta(\mathbf{p}_\Sigma) \delta(\varepsilon_\Sigma) n_2^{(0)} (1 + n_3^{(0)}) (1 + n_4^{(0)}), \quad (26)$$

where

$$p_{3low} = \frac{p_1 + p_2}{2}, \quad p_{3up} = \min(p_1 + p_2, p_c). \quad (27)$$

This rate differs from Eq. (7) in which  $n_2 = n_2^{(0)}$ ,  $n_3 = n_3^{(0)}$ , and  $n_4 = n_4^{(0)}$  by the factor  $(1 + n_1^{(0)})$ . This factor takes into account the creation of phonons that reach the detector. Hence Eq. (26) is more accurate than Eq. (7). However the factor  $(1 + n_1^{(0)})$  is close to 1 for nearly all values of momentum  $p_1$ , except the smallest ones. So both rates [Eqs. (7) and (26)] are practically the same.

In the momentum range where 3pp scattering is allowed, four-phonon process can be represented as two consecutive three-phonon processes. In these processes, the denominators of the matrix elements, in Eq. (12), are resonant. At small angles we can replace terms  $[(E_i - E_Q)^2 + \Gamma_Q^2]^{-1}$  by the delta function  $\pi \delta(E_i - E_Q) / \Gamma_Q$ . As  $\Gamma_Q$  is due to 3pp scattering, it is proportional to the 3pp matrix element. So in essence, the second-order matrix element in Eq. (12) has a numerator with two 3pp matrix elements and the denominator has one 3pp matrix element, so after cancellation the second-order matrix element is equal to one 3pp matrix element.

After a detailed analysis,<sup>8</sup> involving integrating the five resonant matrix elements in Eq. (16) and then summing them, we find that rate of four-phonon processes is equal to the rate of three-phonon processes for the case  $ll1$  when the angles are small. So the scattering process  $ll1$  at small angles can be represented as two consecutive three-phonon processes, with one of them canceling with  $\Gamma$  in the denominator. Also we see that the four-phonon process goes through an intermediate state that is real and not virtual.

We define an “exclusive” four-phonon processes with a rate  $\nu_{exc}$ , which excludes the 4pp scattering that can be represented by 3pp scattering. So  $\nu_{ll1}$  for all angles can be written as

$$\nu_{ll1} = \nu_{3pp} + \nu_{exc}. \quad (28)$$

At larger angles there is only the “exclusive” 4pp type  $ll1$  scattering.

Next we consider the scattering caused by “exclusive” four-phonon processes. Three-phonon processes were studied by us in Refs. 18 and 20. In order to find  $\nu_{exc}$  we integrate over the azimuthal angles of the third- and fourth-phonon  $\varphi_3$ ,  $\varphi_4$ , and variables  $p_4$  and  $\zeta_4$  in Eq. (26), with the help of the  $\delta$  functions of energy and momentum, in a way similar to Refs. 22 and 23. Here and below it will be convenient to use variables  $\zeta_{ij} = 1 - \cos \theta_{ij}$  instead of the angles  $\theta_{ij}$  between phonons with momenta  $\mathbf{p}_i$  and  $\mathbf{p}_j$ . If  $\zeta$  contains only one subscript then the corresponding angle is between the momentum and the anisotropy axis of the system.

In the integration, we exclude the range of variable  $\zeta_2$  where the angle  $\theta_{12}$ , between momenta  $\mathbf{p}_1$  and  $\mathbf{p}_2$ , is less than  $45^\circ$ . We note that though the maximum angle between momenta of phonons, which can participate in a three-phonon process, as dictated by the conservation laws, is equal to  $27^\circ$ , we omit the integration range where  $\theta_{12} \leq 45^\circ$ . This is because there are scatterings in which a phonon, with momentum  $\mathbf{p}_1$ , decays into two in the first 3pp, and in the second 3pp one of these phonons combines with  $\mathbf{p}_2$ . Then there can be angles up to  $45^\circ$  between phonons with momenta  $\mathbf{p}_1$  and  $\mathbf{p}_2$ . So this range of integration excludes the four-phonon process that can be represented as two consecutive three-phonon processes. Consequently, the contribution of the remaining range of integration over angles gives the rate  $\nu_{exc}$  for “exclusive” four-phonon processes.

This procedure underestimates the exclusive 4pp because there can be exclusive 4pp at angles less than  $45^\circ$ . This is not a problem when the angle  $\theta_1$  between the phonon with momentum  $\mathbf{p}_1$  and anisotropy axis  $\mathbf{N}$  of a system is relatively large ( $\theta_1 \geq \frac{\pi}{2}$ ) as then there are practically no phonons in the omitted integration range. This is due to the smallness of  $n_2^{(0)}$  at these angles.

However for small angles  $\theta_1$ , as most of the scattering phonons in the pulse have a small angle to the anisotropy axis, then the omitted integration range would exclude practically all the phonons in the pulse; this can lead to a decrease in the rate of “exclusive” four-phonon processes by several orders of magnitude compared with the true 4pp rate. Therefore such a calculation of the rate of “exclusive” four-phonon processes can only be justified for sufficiently high values of the angle  $\theta_1$ ; i.e.,  $\theta_1 \geq 90^\circ$ .

After integration with the help of the delta functions, further analytic integration of Eq. (26) cannot be precisely made because of the complexity of the integrand. The results of a numerical calculation of the rate  $\nu_{exc}$  for two pulses with parameters  $T_1=0.058$  K,  $\chi_1=0.06$  and  $T_2=0.041$  K,  $\chi_2=0.02$  are shown in Fig. 1 for large angles ( $\theta_1 \geq 90^\circ$ ). The parameters  $T_2$  and  $\chi_2$  correspond to the typical parameters of an  $l$ -phonon pulse that is injected into helium by a heater, while parameters  $T_1$  and  $\chi_1$  correspond to an  $l$ -phonon pulse that initially had parameters  $T_2$  and  $\chi_2$  but has lost energy due to the creation of  $h$  phonons. We note that it would be wrong to state that the pulse was cooled down to temperature  $T_1$  and anisotropy parameter  $\chi_1$  because, as it was shown in Refs. 22 and 23, the temperature of  $l$ -phonon pulse due to the creation of  $h$  phonons increases and does not decrease. However, the value of the anisotropy parameter increases too, so the total energy of  $l$ -phonon pulse decreases, as it must.

The value of the momentum of the relaxing phonon  $p_1$  is chosen to equal the average momentum of phonons in a pulse. For the first pulse, the average momentum of phonons in a pulse is given by  $c\langle p\rangle/k_B=1.28$  K and for second pulse by 1.61 K. Although the qualitative behavior of the rates in both cases is similar, there is nevertheless a strong quantitative difference between the rates at large angles: at  $180^\circ$ , the ratio is  $\approx 12$ ; while at angles about  $90^\circ$ , the ratio is only 2. This difference is due to two factors: first the energy density

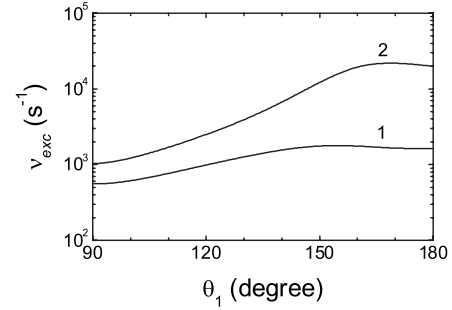


FIG. 1. The angular dependence of the 4pp rate  $\nu_{exc}$ , for the process ( $l_1+l_2 \leftrightarrow l_3+l_4$ ), for different values of the momentum  $p_1$  of the probe phonon, in different scattering pulses. This 4pp rate excludes 4pp scattering, which can be represented by two sequential 3pp. The momentum of the probe  $l$  phonon is taken to be the average phonon momentum  $\langle p \rangle$  in the probe pulse. The probe and scattering pulses are taken to be identical. Curve 1 corresponds to the pulse parameters  $T_1=0.058$  K,  $\chi_1=0.06$ , and  $cp_1/k_B=c\langle p\rangle/k_B=1.28$  K, the scattering pulse at the scattering point, which has lost energy by  $h$ -phonon creation; and curve 2 corresponds to  $T_2=0.041$  K,  $\chi_2=0.02$ , and  $cp_1/k_B=c\langle p\rangle/k_B=1.61$  K, the initial scattering pulse, which has not lost energy by the time it reaches the scattering point.

in the second pulse is twice as large as the first, and second the angular and momentum dependences of the integrand of Eq. (26) are different.

Next we consider the scattering caused by process  $ll2$  [see Eq. (21)]. As the third phonon in this process is an  $h$  phonon and the second and the fourth phonons are  $l$  phonons, then  $n_2=n_2^{(0)}$ ,  $n_3=0$ , and  $n_4=n_4^{(0)}$ . So  $N_b=0$  in this case and the relaxation rate can be obtained from Eq. (7) by substituting the following distribution functions:

$$\nu_{ll2}(\mathbf{p}_1) = \int_{\substack{p_2 \geq p_c - p_1 \\ p_2 \leq p_c}} d^3 p_2 \int_{\substack{p_3 \geq p_c \\ p_3 \leq p_{3up}}} d^3 p_3 \int_{p_4 \leq p_c} d^3 p_4 W(\mathbf{p}_1, \mathbf{p}_2 | \mathbf{p}_3, \mathbf{p}_4) \delta(\mathbf{p}_\Sigma) \delta(\varepsilon_\Sigma) n_2^{(0)} (1 + n_4^{(0)}), \quad (29)$$

where  $p_{3up} = \min(p_1 + p_2, p_{\max})$  and  $p_{\max}$  is the maximum momentum of a phonon. For the calculations we take  $\tilde{p}_{\max} = 20$  K. We note that phonons with momentum more than 14 K do not make a contribution to any of the rates calculated in this paper. Therefore for all values of  $\tilde{p}_{\max} \geq 14$  K the value of the rate is the same.

The integration involving the  $\delta$  functions in Eq. (29) can be made analytically. Further integration can only be precisely made numerically. The results of a numerical calculation of the rate  $\nu_{ll2}$  are shown in Fig. 2.

In Fig. 2 we see that the rate increases monotonically with increasing momentum and monotonically decreases with increasing angle. The physical reasons are that the higher the momentum of the first phonon, the higher is the probability

of  $h$ -phonon creation, and the greater the angle between the two interacting phonons, the smaller is the probability of  $h$ -phonon creation.

Comparison of  $\nu_{exc}$  with  $\nu_{ll2}$ , when  $\theta_1 \geq 90^\circ$ , gives the inequality

$$\nu_{exc}(p_1, \theta_1, T, \chi) \geq \nu_{ll2}(p_1, \theta_1, T, \chi). \quad (30)$$

Inequality (30) shows that the interaction between  $l$ -phonon pulses, at large angles, is mainly due to process  $ll1$  rather than  $ll2$ .

From the calculation of the rates, we can calculate the attenuation coefficient of an  $l$  phonon in an  $l$ -phonon pulse. The attenuation  $A$  is given by

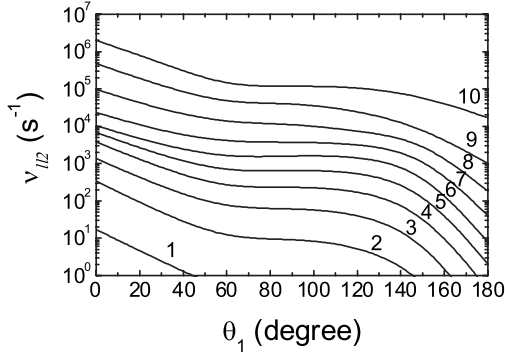


FIG. 2. The angular dependence of the rate  $\nu_{l/2}$ , for the process  $ll2$ , ( $l_1+l_2 \leftrightarrow h_3+l_4$ ), for different values of the momentum of the probe phonon. Curves 1–10 correspond to values of  $cp_1/k_B = 1, 2, \dots, 10$  K, respectively. Calculations are for a scattering pulse with parameters  $T=0.058$  K and  $\chi=0.06$ .

$$A_{ll} = 1 - \exp(-t_{cross}\nu_{exc}). \quad (31)$$

where  $t_{cross}$  is the time of  $l$ -phonon passage through the  $l$ -phonon pulse; it is given by the relation (see Ref. 20)

$$t_{cross} = \frac{t_p}{1 - \cos \alpha} \quad (32)$$

in which  $\alpha$  is the angle between the pulses and  $t_p$  is duration of a current pulse in a heater.

The attenuation coefficient  $A_{ll}$  is calculated for the typical experimental value of pulse duration  $t_p=100$  ns and is shown in Fig. 3. The attenuation coefficient was calculated from Eqs. (31) and (32) and the numerical calculation of the rate  $\nu_{exc}$  (see Fig. 1). In calculations, the angle  $\alpha$  between interacting pulses is considered to be equal to  $\theta_1$  and the momentum  $p_1$  of the scattered phonon is taken to be equal to the average value of the phonon momenta in the probe pulse.

From Fig. 3 it can be seen that the interaction between  $l$ -phonon pulses that have relatively large angles to each other, due to four-phonon processes, is very small and will be hard to detect experimentally. This is in agreement with the results of experiments in which the interaction between  $l$ -phonon pulses was observed only when the angle between them was  $\leq 30^\circ$ .<sup>10</sup> At these small angles there is a very strong interaction due to 3pp.

We note that if we create a pulse with duration equal to 1000 ns the attenuation coefficient will increase ten times in comparison with that shown in Fig. 3. The attenuation coefficient at the interaction point of two pulses with  $T_2=0.041$  K and  $\chi_2=0.02$  moving head-on will be about 1%, which is at the present limit of detection. However for a scattering pulse with  $T_1=0.058$  K and  $\chi_1=0.06$ , which cor-

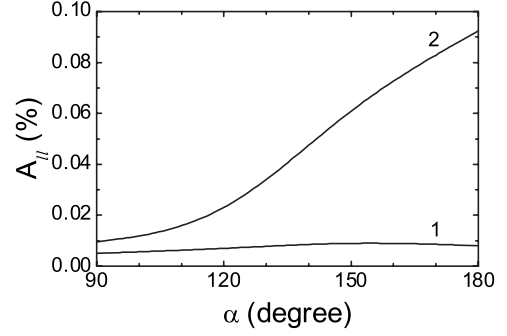


FIG. 3. The angular dependence of the attenuation coefficient  $A_{ll}$  of a probe  $l$ -phonon pulse scattered a second  $l$ -phonon pulse, using the scattering rate  $\nu_{exc}$ . The momentum of the probe  $l$  phonon is taken to be the average phonon momentum  $\langle p \rangle$  in the probe pulse. The probe and scattering pulses are taken to be identical. The angle between them is  $\alpha$ . Curve 1 corresponds to pulse parameters  $T_1=0.058$  K,  $\chi_1=0.06$ , and  $cp_1/k_B=c\langle p \rangle/k_B=1.28$  K; curve 2 corresponds to  $T_2=0.041$  K,  $\chi_2=0.02$ , and  $cp_1/k_B=c\langle p \rangle/k_B=1.61$  K. The calculations were made for pulses with pulse duration  $t_p=100$  ns.

respond to an  $l$ -phonon pulse that practically does not create  $h$  phonons, to get an attenuation equal to 1%, with an angle between pulses equal to  $150^\circ$ , would need the duration of a pulse to be  $10^{-5}$  s. This is very long; it is a quarter of the  $l$ -phonon flight time for a path length of 10 mm. We conclude that it will be difficult to observe the attenuation of a probe of  $l$  phonons by a scattering pulse of  $l$  phonons due to 4pp, which exclude equivalent 3pp.

#### IV. $h$ - $l$ PHONON SCATTERING

In this section we consider the problem of the interaction between one  $h$  phonon and a pulse of  $l$  phonons. The attenuation of a probe  $h$ -phonon pulse by an  $l$ -phonon pulse has been measured.<sup>10</sup> There are three types of scattering with 0, 1, or 2  $h$  phonons being created,

$$\begin{aligned} h_1 + l_2 &\leftrightarrow l_3 + l_4 \quad (\text{type } hl1), \\ h_1 + l_2 &\leftrightarrow h_3 + l_4 \quad (\text{type } hl2), \\ h_1 + l_2 &\leftrightarrow h_3 + h_4 \quad (\text{type } hl3). \end{aligned} \quad (33)$$

We begin with the process  $hl1$ , i.e., the scattering of an  $h$  phonon by an  $l$ -phonon pulse with the creation of two  $l$  phonons. The scattering rate  $\nu_{hl1}$  is given by Eq. (7). The distribution functions of  $l$  phonons in Eq. (7) ( $n_2$ ,  $n_3$ , and  $n_4$ ) are the equilibrium ones [see Eq. (23)] as  $l$  phonons in a pulse quickly come to equilibrium by 3pp scattering. So the rate  $\nu_{hl1}$  can be written as

$$\nu_{hl1}(\mathbf{p}_1) = \int_{p_2 \leq 2p_c - p_1} d^3 p_2 \int_{\substack{p_{3low} \leq p_3 \\ p_3 \leq p_c}} d^3 p_3 \int_{p_4 \leq p_3} d^3 p_4 W(\mathbf{p}_1, \mathbf{p}_2 | \mathbf{p}_3, \mathbf{p}_4) \delta(\mathbf{p}_\Sigma) \delta(\varepsilon_\Sigma) n_2^{(0)} (1 + n_3^{(0)}) (1 + n_4^{(0)}), \quad (34)$$

where  $p_{3low}$  is defined by Eq. (27).

According to Eq. (6) the relation for  $N_d$  can be written as

$$N_d = n_1 \nu_{hl1}. \quad (35)$$

At small angles between the pulses, it is possible that an  $h$  phonon is created in the scattering pulse of  $l$  phonons, and this  $h$  phonon will reach the detector. This would look like an increase in the  $h$ -phonon probe signal. We now consider the rate of  $h$ -phonon creation,  $N_b$ , in the  $l$ -phonon pulse and the size of such a signal.

Taking into account the equality

$$n_3^{(0)} n_4^{(0)} (1 + n_2^{(0)}) = e^{-(\varepsilon_1 - \mathbf{p}_1 \mathbf{u}) / (k_B T)} n_2^{(0)} (1 + n_3^{(0)}) (1 + n_4^{(0)}), \quad (36)$$

which follows from Eq. (23) and the conservation laws, we derive

$$N_b = e^{-(\varepsilon_1 - \mathbf{p}_1 \mathbf{u}) / (k_B T)} (1 + n_1) \nu_{hl1}. \quad (37)$$

In short pulses, which were used in experiments, any created  $h$  phonons are left behind by the  $l$  phonons, and the number of phonons with  $p_1$  in the scattering pulse,  $n_1$ , is much less than the unity. Therefore for short pulses (we only consider short scattering pulses in this section) we have the relation

$$N_b^{(sh)} = e^{-(\varepsilon_1 - \mathbf{p}_1 \mathbf{u}) / (k_B T)} \nu_{hl1}. \quad (38)$$

At small angles between the anisotropy axis and the momentum, the exponential term in Eq. (38) is about unity. So  $N_b^{(sh)} \gg N_d$  and the first term on the right-hand part of Eq. (2) is much greater than the second, which can be neglected in this case. Thus the kinetic equation becomes

$$\frac{dn_1}{dt} = N_b^{(sh)}. \quad (39)$$

In this case,  $hl1$ , we might expect an increase in the signal and not an attenuation. However by the time the scattering pulse has reached the intersection point with the probe pulse, it will have such a low energy that it has almost stopped creating  $h$  phonons. When this happens we do not expect any change in the probe  $h$ -phonon signal. This is in good agreement with experiment<sup>10</sup> where no attenuation is seen at angles 30 and 40°.

The situation is quite different at large angles between the momentum of the  $h$  phonon and the anisotropy axis of the  $l$ -phonon pulse; i.e.,  $\theta_1 \geq 90^\circ$ . In this case the exponential factor in  $N_b$  becomes very small and the kinetic equation (2) can be written as

$$\frac{dn_1}{dt} = -N_d = -n_1 \nu_{hl1}. \quad (40)$$

So we have a process for  $h$ -phonon scattering in an

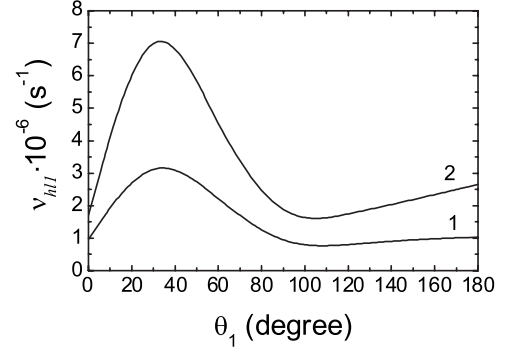


FIG. 4. The angular dependence of the rate  $\nu_{hl1}$  of process  $hl1$ , ( $h_1 + l_2 \leftrightarrow l_3 + l_4$ ), for different values of the scattering pulse. The momentum of the probe phonon is taken as  $cp_1/k_B = 10$  K. Curve 1 corresponds to the scattering pulse parameters  $T_1 = 0.058$  K and  $\chi_1 = 0.06$ , the scattering pulse at the scattering point that has lost energy by  $h$ -phonon creation, and curve 2 corresponds to  $T_2 = 0.041$  K and  $\chi_2 = 0.02$ , the initial scattering pulse that has not lost energy by the time it reaches the scattering point.

anisotropic  $l$ -phonon system. We see that the scattering rate is exactly equal to  $\nu_{hl1}$ .

The momentum and angular dependences of the rate  $\nu_{hl1}$  were obtained by us in Refs. 22 and 23, where the physical reasons for these dependences have also been analyzed. The scattering rate  $\nu_{hl1}$  of  $h$  phonon with momentum  $cp_1/k_B = 10$  K in an  $l$ -phonon pulse with parameters  $T_1 = 0.058$  K and  $\chi_1 = 0.06$  and  $T_2 = 0.041$  K and  $\chi_2 = 0.02$  was calculated from Eq. (34) and is shown in Fig. 4. One can see that an  $l$ -phonon pulse with  $T_1 = 0.058$  K and  $\chi_1 = 0.06$  has rates that are  $\sim 2$  times smaller than for a pulse with  $T_2 = 0.041$  K and  $\chi_2 = 0.02$ . We note that the initial values of the parameters of  $T_2 = 0.041$  K and  $\chi_2 = 0.02$  roughly correspond to a heater power of 25 mW.

Although the rate  $\nu_{hl1}$  only changes  $\sim 2$  times between the two pulses, the change in the parameters of the pulse has a large influence on  $h$ -phonon creation. It was shown by us in Refs. 22 and 23 that the  $l$ -phonon pulse, with parameters  $T_2 = 0.041$  K and  $\chi_2 = 0.02$ , intensively creates  $h$  phonons, but in a pulse with  $T_1 = 0.058$  K and  $\chi_1 = 0.06$  there is practically no  $h$ -phonon creation. This difference can be explained by the fact that Eq. (39) not only depends on the rate  $\nu_{hl1}$  in the pulse, which weakly changes with the pulse parameters, but also depends on the exponential factor on the right-hand side of Eq. (38). This factor changes approximately 170 times between the two sets of pulse parameters. Thus,  $N_b^{(sh)}$  changes  $\approx 340$  times; this means that there is practically no  $h$ -phonon creation in a pulse with  $T_1 = 0.058$  K and  $\chi_1 = 0.06$ . The distribution function for the  $l$  phonons in the pulse, which enters into the rate  $\nu_{hl1}$ , only changes  $\approx 3$  times between the pulses. So this leads to the weak change in the rate  $\nu_{hl1}$ .

We now consider the rate due to the second process  $\nu_{hl2}$ . This can be derived from Eq. (7), where  $n_3 = 0$  as there are no  $h$  phonons in the  $l$ -phonon pulse and  $n_2 = n_2^{(0)}$  and  $n_4 = n_4^{(0)}$  are the distribution functions for  $l$  phonons in the pulse



$$\nu_{hl2}(\mathbf{p}_1) = \int_{p_2 \leq p_c} d^3 p_2 \int_{\substack{p_{3low} \leq p_3 \\ p_3 \leq p_{3up}}} d^3 p_3 \int_{p_4 \leq p_c} d^3 p_4 W(\mathbf{p}_1, \mathbf{p}_2 | \mathbf{p}_3, \mathbf{p}_4) \delta(\mathbf{p}_\Sigma) \delta(\varepsilon_\Sigma) n_2^{(0)} (1 + n_4^{(0)}), \quad (41)$$

where  $p_{3low} = \max(p_c, p_1 + p_2 - p_c)$  and  $p_{3up} = \min(p_1 + p_2, p_{max})$ .

The results of calculation of the rate  $\nu_{hl2}$  from Eq. (41) are shown in Fig. 6. At once we see that this process will not lead to an observable attenuation of a pulse as it does not lead to any significant exchange of energy between  $l$ - and  $h$ -phonon subsystems.

We note that the rate  $\nu_{hl1}(\tilde{p}_1=10 \text{ K}, \theta_1)$  is the same as  $\nu_{hl2}(\tilde{p}_1=10 \text{ K}, \theta_1)$  (see Figs. 2 and 5, respectively) as at  $\tilde{p}_1 = 10 \text{ K}$  it is the same relaxation rate.

Relation (41) for the rate  $\nu_{hl2}$  is formally similar to Eq. (34) for the rate  $\nu_{hl1}$  although the numerical values and dependences of these rates appear quite different. The different momentum and angular dependences of the rates  $\nu_{hl1}$  and  $\nu_{hl2}$  are determined first by the different limits of integration on  $p_2$  and  $p_3$  and second by the probability densities  $W$ , which behave differently as a function of momentum.

The rate of the third process  $\nu_{hl3}$  can be derived from Eq. (7), with  $n_3=0$  and  $n_4=0$ , as there are no  $h$  phonons in  $l$ -phonon pulse, and  $n_2=n_2^{(0)}$  is the distribution functions of  $l$  phonons in the scattering pulse

$$\nu_{hl3}(\mathbf{p}_1) = \int_{\substack{p_2 \geq 2p_c - p_1 \\ p_2 \leq p_c}} d^3 p_2 \int_{\substack{p_3 \geq p_{3low} \\ p_3 \leq p_{3up}}} d^3 p_3 \int_{\substack{p_4 \leq p_3 \\ p_4 \geq p_c}} d^3 p_4 W(\mathbf{p}_1, \mathbf{p}_2 | \mathbf{p}_3, \mathbf{p}_4) \delta(\mathbf{p}_\Sigma) \delta(\varepsilon_\Sigma) n_2^{(0)}, \quad (42)$$

where  $p_{3low}$  is defined by Eq. (27) and  $p_{3up} = p_1 + p_2 - p_c$ .

The results of the calculation of the rate  $\nu_{hl3}$  from Eq. (42) are shown in Fig. 5. As expected, the rate of type  $hl3$  process is less than the rate of the second type  $\nu_{hl2}$  because the probability of creating two  $h$  phonons is less than the probability of creating one  $h$  phonon and one  $l$  phonon. The momentum and angular dependences of the rate  $\nu_{hl3}$  are mainly defined by the angular and momentum dependences of the probability density and the distribution functions.

The rates of these  $h$ - $l$  processes have been calculated in the Bose-cone approximation for  $\theta_1=0$  in Ref. 21. The calculated rates for the  $hl1$  scattering are in good agreement. The rates for the other two processes differ from the results obtained here. These differences are due first to the fact that the approximate matrix element was used in Ref. 21 and second that the approximate Bose-cone distribution function was used.

From the rates calculated here we see that the interaction between  $h$ - and  $l$ -phonon pulses is mainly due to the  $hl1$  process. The attenuation coefficient of  $h$  phonons in  $l$ -phonon pulse at large values of the angle can be written as

$$A = 1 - \exp(-t_{cross} \nu_{hl1}), \quad (43)$$

where  $t_{cross}$  is the crossing time of an  $h$ -phonon probe pulse through the  $l$ -phonon scattering pulse, which is given by [compare with Eq. (32)]

$$t_{cross} = \frac{ct_p}{c - v_c \cos \alpha}. \quad (44)$$

Here  $\alpha$  is the angle between pulses;  $v_c = 189 \text{ m/s}$  is a group velocity of  $h$  phonon with energy equal to 10 K.

For  $\alpha = 160^\circ$  we calculate the attenuation coefficient from Eqs. (43) and (44) and from the calculated rate  $\nu_{hl1}$ . The angle  $\alpha$  between the interacting pulses is taken to be equal to the angle  $\theta_1$ . The momentum  $p_1$  of the scattered  $h$  phonon is taken to be equal to the average momentum of phonons in the  $h$ -phonon pulse. The rate for this case is equal to  $\nu_1 = 1.15 \times 10^6 \text{ s}^{-1}$ ,  $t_{cross} = 5.7 \times 10^{-7} \text{ s}$ , and  $t_p = 1000 \text{ ns}$ . This gives an attenuation coefficient of  $A = 48\%$ . This is in reasonable agreement with experiment in which 30% attenuation was observed at  $\alpha = 160^\circ$ . The calculated attenuation is a little higher than that measured, but in the calculation we have not counted phonons that are created in the scattering process. Some of these scattered phonons will reach the detector. For shorter pulse ( $t_p = 100 \text{ ns}$ ) we calculate  $A = 6.4\%$ , while in the experiment 3% attenuation is observed.

## V. $h$ - $h$ PHONON SCATTERING

As in the previous sections we model the interaction between two  $h$ -phonon pulses by considering one  $h$ -phonon scattering in a cloud of  $h$  phonons. The scattering can happen in two ways,

$$h_1 + h_2 \leftrightarrow h_3 + l_4 \quad (\text{type } hh1),$$

$$h_1 + h_2 \leftrightarrow h_3 + h_4 \quad (\text{type } hh2). \quad (45)$$

The rate for the first of the processes in expression (45) can be obtained by substituting  $n_2 = n_{2h}^{(0)}$ ,  $n_3 = n_{3h}^{(0)}$ , and  $n_4 = 0$  in Eq. (7),

$$\nu_{hh1}(\mathbf{p}_1) = \int_{\substack{p_c \leq p_2 \\ p_2 \leq p_{2up}}} d^3 p_2 \int_{\substack{p_{3low} \leq p_3 \\ p_3 \leq p_{3up}}} d^3 p_3 \int_{p_4 \leq p_c} d^3 p_4 W(\mathbf{p}_1, \mathbf{p}_2 | \mathbf{p}_3, \mathbf{p}_4) \delta(\mathbf{p}_\Sigma) \delta(\varepsilon_\Sigma) n_{2h}^{(0)} (1 + n_{3h}^{(0)}), \quad (46)$$

where  $p_{3low}$ ,  $p_{3up}$ , and  $p_{2up}$  are defined by

$$\begin{aligned} p_{3low} &= \min(p_1 + p_2 - p_c, p_{\max}), \\ p_{3up} &= \min(p_1 + p_2, p_{\max}), \\ p_{2up} &= p_c + p_{\max} - p_1. \end{aligned} \quad (47)$$

In Eq. (46)  $n_{ih}^{(0)}$  is the distribution function for  $h$  phonons in the scattering pulse of  $h$  phonons. The integration, in expression (46), using the  $\delta$  functions can be made in a similar way to the previous sections.

In order to numerically integrate Eq. (46) we need the distribution function for the  $h$  phonons. The distribution function for  $h$  phonons in a pulse, which was created by a pulse of  $l$  phonons, was derived in the Bose-cone approximation in Ref. 30. It can be written as

$$\begin{aligned} n_h^{(0)}(p, \zeta, z, t) &= \frac{c t_p A_1}{c - v_p} \frac{e^{-A_2/T(t_b)}}{e^{\varepsilon(p)/k_B T(t_b)} - 1} e^{-A_3[c(p-p_c)/k_B]} \eta(t \\ &\quad - t_b) \eta(t_b) \eta(\zeta_p^{(h)} - \zeta). \end{aligned} \quad (48)$$

where  $A_1 = 1.228 \times 10^9 \text{ s}^{-1}$ ,  $A_2 = 3.188 \text{ K}$ ,  $A_3 = 1.65 \text{ K}^{-1}$ ,  $v_p$  is the group velocity of  $h$  phonons with momentum  $p$ ,  $t_p$  is a duration of the current pulse in the heater that is taken as 100 ns, and  $\zeta_p^{(h)} = 1 - \cos \theta_p^{(h)}$ , where  $\theta_p^{(h)}$  is the typical half-angle of the cone occupied by the  $h$  phonons in momentum space, which is  $4^\circ$  (Refs. 11, 22, 23, and 31),

$$t_b = \frac{z - v_p t}{c - v_p}, \quad (49)$$

and the function  $T(t_b)$  is defined by the relation

$$\overline{\frac{\nu_{b1}(T)}{T^4}} e^{-\varepsilon_c/k_B T} = \frac{\overline{\nu_{b1}(T_0)}}{T_0^4} e^{-\varepsilon_c/k_B T_0} \left(1 + \frac{t_b}{\tau_S}\right)^{-1}. \quad (50)$$

In Eq. (50),  $T_0$  is the initial temperature of the  $l$ -phonon pulse that is taken to be 1 K,  $\varepsilon_c/k_B = 10 \text{ K}$ ,

$$\tau_S = \frac{4 \pi^4 k_B^3 T_0^3 v_c e^{\varepsilon_c/k_B T_0}}{15 c \varepsilon_c^3 \nu_{b1}(T_0)} \frac{T_0}{\varepsilon_c/k_B + A_2}, \quad (51)$$

and

$$\overline{\nu_{b1}(T)} = A_1 e^{-A_2/T} \left(1 + A_3 \frac{c}{v_c} T\right)^{-1}. \quad (52)$$

The  $h$  phonons have momenta close to  $p_c$  in such a pulse.

Distribution function (48) enables us to calculate the density of high-energy phonons, created by a pulse of low-energy phonons, at any point  $z$  and at any time  $t$ . To calculate the rate of interaction, we need the distribution function of  $h$  phonons at the point where the  $h$ -phonon pulses intersect. This point determines the time of their intersection. As the distance between the heater, which creates the scattering pulse, and the point of intersection in the experiments, was equal to 10 mm, so  $z = 10 \text{ mm}$ . The time was chosen so that the energy density of  $h$  phonons at point  $z$  was maximized. As it was shown in Ref. 30 that this time can be found from the relation  $t = z/v_c \approx 52.9 \text{ } \mu\text{s}$ .

The results of the numerical calculation of the rate  $\nu_{hh1}$  from Eq. (46) with the distribution function of  $h$  phonons given by Eq. (48) at  $z = 10 \text{ mm}$  and  $t = 52.9 \text{ } \mu\text{s}$  are shown in Fig. 7. The angular and momentum dependences of the rate  $\nu_{hh1}$  are determined by a probability density  $W$  that enters into the integrand and by the distribution function of  $h$  phonons  $n_{2h}^{(0)}$ .

Now we consider the second process,  $hh2$ , from Eq. (45). The scattering rate  $\nu_{hh2}$  from Eq. (7) is equal to

$$\nu_{hh2}(\mathbf{p}_1) = \int_{\substack{p_2 \geq p_c \\ p_2 \leq p_{\max}}} d^3 p_2 \int_{\substack{p_3 \geq p_{3low} \\ p_3 \leq p_{3up}}} d^3 p_3 \int_{\substack{p_4 \geq p_c \\ p_4 \leq p_3}} d^3 p_4 W(\mathbf{p}_1, \mathbf{p}_2 | \mathbf{p}_3, \mathbf{p}_4) \delta(\mathbf{p}_\Sigma) \delta(\varepsilon_\Sigma) n_{2h}^{(0)} (1 + n_{3h}^{(0)}) (1 + n_{4h}^{(0)}). \quad (53)$$

Here  $p_{3low}$  is defined by Eq. (27) and  $p_{3up} = \min(p_1 + p_2, p_{\max})$ . We note that for this case there is also a creation process that will make real relaxation rate a little smaller compared to that from Eq. (53). The results of the numerical calculation of the rate  $\nu_{hh2}$  from Eq. (53) are shown in Fig. 8.

As  $h$  phonons in a pulse have momenta close to  $p_c$ , the process  $hh1$  appears much more effective than process  $hh2$

for  $h$ -phonon pulses interacting at any angle between them. We conclude that  $h$ -phonon pulses interact mainly due to the process  $hh1$ .

Using our calculation of the rates, we estimate the attenuation of the probe  $h$ -phonon signal scattered by an  $h$ -phonon pulse, through the  $hh1$  process. It can be written as

$$A = 1 - \exp(-t_{cross}\nu_{hl1}), \quad (54)$$

where  $t_{cross}$  is time for the probe  $h$  phonon to cross the scattering  $h$ -phonon pulse,<sup>10</sup>

$$t_{cross} = \frac{t_h}{\sin \alpha}. \quad (55)$$

Here  $\alpha$  is the angle between the pulses, and  $t_h = 2.25 \times 10^{-6}$  s is the time corresponding to a spatial half-width of  $h$ -phonon signal, which can be estimated from Ref. 30.

The attenuation coefficient, calculated from Eqs. (54) and (55) for  $\alpha = 30^\circ$ , and the results of numerical calculation of the rate  $\nu_{hl1}$  are shown in Fig. 7. The angle  $\alpha$  between interacting pulses is taken to be equal to the angle  $\theta_1$ , and the momentum  $p_1$ , of the probe phonon, is taken as equal to the average value of momentum of phonons in the probe pulse,  $cp_1/k_B = c\langle p \rangle/k_B = 10$  K. The rate for this case is equal to  $\nu_{hl1}(cp_1/k_B = 10 \text{ K}, \theta_1 = 30^\circ) = 3.02 \times 10^4 \text{ s}^{-1}$ ,  $t_{cross} = 4.5 \times 10^{-6}$  s and the attenuation coefficient is  $A = 12.7\%$ . This is in reasonable agreement with experiment where 4.5% attenuation is observed at  $\alpha = 30^\circ$ . The calculated rate is overestimated as first that the some of the scattered phonons will reach the detector and second we that have assumed that the distribution function of  $h$  phonons is constant over the volume where the pulses intersect. The actual spatial inhomogeneity of distribution function will decrease the attenuation. Also if the initial temperature  $T_0$  of the initial  $l$ -phonon pulse is less than 1 K, as is found in some experiments,<sup>32</sup> the density of  $h$  phonons in the scattering pulse is smaller, and the calculated attenuation will be smaller.

## VI. CONCLUSION

The rate of four-phonon scattering in liquid helium, for phonons of all momenta, is found from the kinetic equation [Eq. (7)]. When three-phonon processes are allowed, particular care must be taken in calculating the 4pp rate. For the range of momenta where 3pp are allowed, the 4pp matrix elements [Eq. (16)] have resonances when the angle between the two interacting phonon momenta is small. This is because the denominators of the matrix element can be zero when three-phonon processes are allowed, and the intermediate states, in second-order perturbation theory, are real rather than virtual. This problem is resolved by realizing that the intermediate states have finite lifetimes due to 3pp scattering so their energies are complex rather than real. This replaces the infinities with delta functions, and the 4pp scattering rates can then be calculated.

In the angular range, where three-phonon processes are permitted, the rate of four-phonon processes is very close to the rate of three-phonon processes. This is because the 4pp is equivalent to two sequential 3pps, so the 3pp and 4pp rates should not be added together. In this angular and momentum range, the 4pp scattering rates are very high because they are essentially 3pp rates. At larger angles, 3pps are not allowed as energy and momentum cannot be conserved, and the 4pp cannot be considered as two 3pps. The 4pp scattering rate is then relatively very low. We call this the 4pp exclusive rate at it excludes the equivalent 3pp scattering, and it is given in Eqs. (26) and (28).

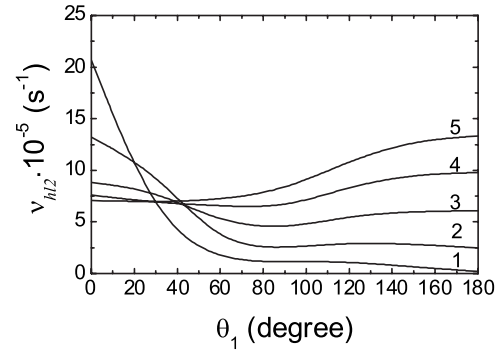


FIG. 5. The angular dependences of the rate  $\nu_{hl2}$  for type  $hl2$  process,  $(h_1+l_2 \leftrightarrow h_3+l_4)$ , for different values of the momentum of the probe  $h$  phonon. Curves 1–5 correspond to values of  $cp_1/k_B = 10, 11, 12, 13,$  and  $14$  K, respectively. Calculations were made for a scattering  $l$ -phonon pulse with parameters  $T = 0.058$  K and  $\chi = 0.06$ .

The problem of the interaction between two  $l$ -phonon pulses, due to exclusive four-phonon processes, is solved for large angles between pulses. It is shown that there are two processes,  $ll1$  and  $ll2$ , for this interaction [see Eq. (21)]. The rates of these processes are calculated and shown in Figs. 1 and 2. The process  $ll1$ , where two  $l$  phonons are created, is much more effective than process  $ll2$  where one  $l$  phonon and one  $h$  phonon are created.

The attenuation coefficient of a probe  $l$ -phonon pulse due to its interaction with a scattering  $l$ -phonon pulse is calculated and is shown in Fig. 3. From the results of the calculated attenuation coefficient we see that there should be no experimentally observed attenuation due to the interaction of  $l$ -phonon pulses at large angles, certainly for  $\alpha \geq 90^\circ$  and probably for smaller angles down to  $\alpha \sim 45^\circ$ . This is in agreement with the experimental results in Ref. 10 for  $\alpha = 40^\circ$  in which no attenuation was detected. The measured attenuation at  $\alpha = 30^\circ$  is essentially due to 3pp scattering (see Refs. 17 and 18), and as the angle  $\alpha$  decreases below  $30^\circ$ , the attenuation rapidly increases and becomes immeasurably large.

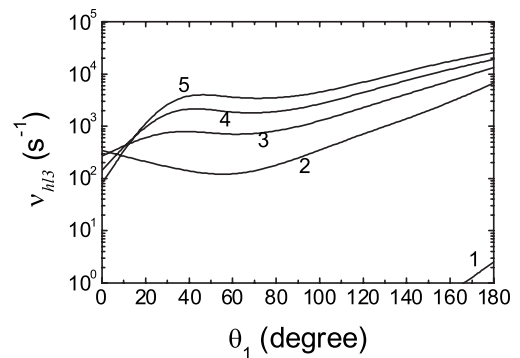


FIG. 6. The angular dependence of the rate  $\nu_{hl3}$  for type  $hl3$  process,  $(h_1+l_2 \leftrightarrow h_3+h_4)$ , for different values of the probe  $h$ -phonon momentum. Curves 1–5 correspond to values of  $cp_1/k_B = 10, 11, 12, 13,$  and  $14$  K, respectively. Calculations were made for a scattering  $l$ -phonon pulse with parameters  $T = 0.058$  K and  $\chi = 0.06$ .

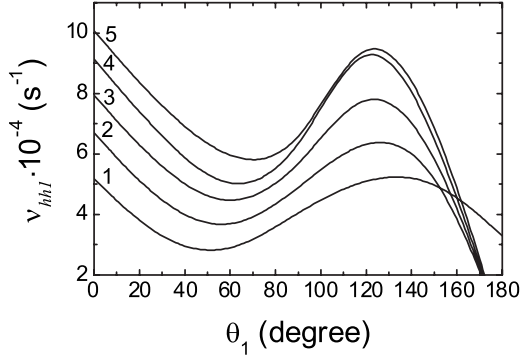


FIG. 7. The angular dependence of the rate  $\nu_{hh1}$  for type  $hh1$  process, ( $h_1+h_2 \leftrightarrow h_3+l_4$ ), for different values of the momentum of the probe  $h$  phonon. Curves 1–5 correspond to values of  $cp_1/k_B = 10, 11, 12, 13,$  and  $14$  K accordingly. The initial temperature  $T_0$  of  $l$ -phonon pulse, which has created the scattering  $h$ -phonon pulses, is equal to  $1$  K in the Bose-cone approximation; the solid angle occupied by the scattering  $h$ -phonon pulse in momentum space is  $\Omega_p^{(h)} = 1.53 \times 10^{-2}$  sr.

The problem of interactions between  $h$ - and  $l$ -phonon pulses is then considered. It is shown that this relaxation can be caused by three different processes [Eq. (33)]. The rates all of three processes are found (see Figs. 4–6). We find that generally the process  $h+l \rightarrow l+l$  is stronger than  $h+l \rightarrow l+h$ , which is stronger than  $h+l \rightarrow h+h$ . This is due to the extra energy required to create an  $h$  phonon rather than an  $l$  phonon. At large angles between the pulses, the interaction between  $h$ - and  $l$ -phonon pulses is due only to the first ( $hl1$ ) process. The calculated attenuation coefficient of a probe  $h$ -phonon pulse scattered by an  $l$ -phonon pulse is 48%, which is in good agreement with experimental attenuation of 30% (Ref. 10) at  $\alpha = 160^\circ$ .

The interaction between two  $h$ -phonon pulses is then considered. It is shown that there are two processes for this interaction [see Eq. (45)]. We find that generally the process  $h+h \rightarrow h+l$  is stronger than  $h+h \rightarrow h+h$ . The rates for both processes are calculated (see Figs. 7 and 8). The interaction between two  $h$ -phonon pulses is mainly due to the first process  $hh1$  rather than the second  $hh2$ . The calculated attenuation coefficient of a probe  $h$ -phonon pulse scattered by an  $h$ -phonon pulse at  $\alpha = 30^\circ$  is 12.7%. This is reasonable agreement with experimental attenuation of 4.5% (Ref. 10) as there are no adjustable constants. The reasons for the difference are discussed.

In conclusion we have shown that the 4pp scattering rates in liquid  $^4\text{He}$ , calculated from first principles, give attenuation coefficients that are in reasonable agreement with the directly measured scattering rates. We conclude that we can satisfactorily calculate all the main phonon-phonon scattering processes in liquid He II, 3pp in Refs. 17 and 18, and 4pp in this paper.

#### ACKNOWLEDGMENTS

We are grateful to the EPSRC-GB (Grant No. EP/F019157/1) for support of this work.

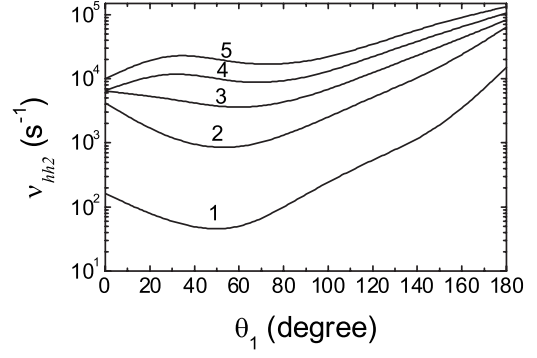


FIG. 8. The angular dependence of the rate  $\nu_{hh2}$  for type  $hh2$  process, ( $h_1+h_2 \leftrightarrow h_3+h_4$ ), for different values of momentum of the probe  $h$  phonon. Curves 1–5 correspond to the values of  $cp_1/k_B = 10, 11, 12, 13,$  and  $14$  K, accordingly. The initial temperature  $T_0$  of  $l$ -phonon pulse that has created  $h$ -phonon pulse is equal to  $1$  K in the Bose-cone approximation; the solid angle occupied by the scattering  $h$ -phonon pulse in momentum space is  $\Omega_p^{(h)} = 1.53 \cdot 10^{-2}$  sr.

#### APPENDIX: RELATIONSHIPS BETWEEN THE ANGLES FOR THE MATRIX ELEMENT

Having expanded the dot products in Eqs. (17)–(20) and taking conservation laws of energy and momentum (1) into account, we have

$$M^{(1)} = \frac{\varepsilon_{1+2}}{\varepsilon_{1+\varepsilon_2-\varepsilon_{1+2}+i\Gamma^{(1)}}} \left[ 2u - \zeta_{12} + \frac{p_1+p_2}{p_{1+2}} (2 - \zeta_{12}) \right] \left[ 2u - \zeta_{34} + \frac{p_3+p_4}{p_{1+2}} (2 - \zeta_{34}) \right], \quad (\text{A1})$$

$$M^{(5)} = - \frac{\varepsilon_{1+2}}{\varepsilon_{1+\varepsilon_2+\varepsilon_{1+2}}} \left[ 2u - \zeta_{12} - \frac{p_1+p_2}{p_{1+2}} (2 - \zeta_{12}) \right] \left[ 2u - \zeta_{34} - \frac{p_3+p_4}{p_{1+2}} (2 - \zeta_{34}) \right], \quad (\text{A2})$$

$$M_{13}^{(3)} = \frac{\varepsilon_{1-3}}{\varepsilon_{1-\varepsilon_3-\varepsilon_{1-3}+i\Gamma^{(13)}}} \left[ 2u - \zeta_{13} + \frac{p_1-p_3}{p_{1-3}} (2 - \zeta_{13}) \right] \left[ 2u - \zeta_{24} + \frac{p_4-p_2}{p_{1-3}} (2 - \zeta_{24}) \right], \quad (\text{A3})$$

$$M_{24}^{(3)} = \frac{\varepsilon_{2-4}}{\varepsilon_{2-\varepsilon_4+\varepsilon_{2-4}+i\Gamma^{(24)}}} \left[ 2u - \zeta_{13} + \frac{p_3-p_1}{p_{1-3}} (2 - \zeta_{13}) \right] \left[ 2u - \zeta_{24} + \frac{p_2-p_4}{p_{1-3}} (2 - \zeta_{24}) \right], \quad (\text{A4})$$

$$M_{14}^{(3)} = \frac{\varepsilon_{1-4}}{\varepsilon_{1-\varepsilon_4-\varepsilon_{1-4}+i\Gamma^{(14)}}} \left[ 2u - \zeta_{14} + \frac{p_1-p_4}{p_{1-4}} (2 - \zeta_{14}) \right] \left[ 2u - \zeta_{23} + \frac{p_3-p_2}{p_{1-4}} (2 - \zeta_{23}) \right], \quad (\text{A5})$$

$$M_{23}^{(3)} = \frac{\varepsilon_{2-3}}{\varepsilon_{2-\varepsilon_3+\varepsilon_{2-3}+i\Gamma^{(23)}}} \left[ 2u - \zeta_{14} + \frac{p_4-p_1}{p_{1-4}} (2 - \zeta_{14}) \right] \left[ 2u - \zeta_{23} + \frac{p_2-p_3}{p_{1-4}} (2 - \zeta_{23}) \right]. \quad (\text{A6})$$

Here variables  $\zeta_{ij}$  are given by relation  $\zeta_{ij} = 1 - \cos \theta_{ij}$ , where  $\theta_{ij}$  is the angle between phonons with momenta  $\mathbf{p}_i$  and  $\mathbf{p}_j$ ,  $\varepsilon_{i\pm j} = \varepsilon(p_{i\pm j})$ , and

$$p_{i+j} = \sqrt{(p_i + p_j)^2 - 2p_i p_j \zeta_{ij}}, \quad p_{i-j} = \sqrt{(p_i - p_j)^2 + 2p_i p_j \zeta_{ij}}. \quad (\text{A7})$$

From the energy and momentum conservation laws, the following relations between the angles can be obtained:

$$\zeta_{34} = \frac{(p_3 + p_4)^2 - (p_1 + p_2)^2 + 2p_1 p_2 \zeta_{12}}{2p_3 p_4}, \quad (\text{A8})$$

$$\zeta_{23} = \frac{(p_1 - p_4)^2 - (p_2 - p_3)^2 + 2p_1 p_4 \zeta_{14}}{2p_2 p_3}, \quad (\text{A9})$$

$$\zeta_{24} = \frac{(p_1 - p_3)^2 - (p_2 - p_4)^2 + 2p_1 p_3 \zeta_{13}}{2p_2 p_4}, \quad (\text{A10})$$

where

$$\zeta_{1i} = \zeta_1 + \zeta_i - \zeta_1 \zeta_i - \sqrt{2\zeta_1 - \zeta_1^2} \sqrt{2\zeta_i - \zeta_i^2} \cos(\varphi_i - \varphi_1). \quad (\text{A11})$$

In Eq. (A11), the angles  $\varphi_i$  are the azimuth angles of phonons with momentum  $\mathbf{p}_i$  relative to the  $x$  axis, which is perpendicular to the anisotropy axis, and  $\zeta_i = 1 - \cos \theta_i$ , where  $\theta_i$  is the angle between the momentum  $\mathbf{p}_i$  and the anisotropy axis of the system.

\*a.f.g.wyatt@exeter.ac.uk

<sup>1</sup>L. Landau, J. Phys. (USSR) **5**, 71 (1941).

<sup>2</sup>I. M. Khalatnikov, *An Introduction to the Theory of Superfluidity* (Addison-Wesley, New York, 1989).

<sup>3</sup>L. Tisza, Nature (London) **141**, 913 (1938).

<sup>4</sup>F. Mezei, C. Lartigue, and B. Farago, in *Excitations in Two Dimensional and Three Dimensional Quantum Fluids*, edited by A. F. G. Wyatt and H. J. Lauter (Plenum Press, New York, 1991), p. 119.

<sup>5</sup>D. G. Henshaw and A. D. B. Woods, Phys. Rev. **121**, 1266 (1961).

<sup>6</sup>O. W. Dietrich, E. H. Graph, C. H. Huang, and L. Passell, Phys. Rev. A **5**, 1377 (1972).

<sup>7</sup>L. D. Landau and I. M. Khalatnikov, Zh. Eksp. Teor. Fiz. **19**, 637 (1949).

<sup>8</sup>I. N. Adamenko, Yu. A. Kitsenko, K. E. Nemchenko, and A. F. G. Wyatt, Fiz. Nizk. Temp. **35**, 265 (2009).

<sup>9</sup>H. J. Maris and W. E. Massey, Phys. Rev. Lett. **25**, 220 (1970).

<sup>10</sup>D. H. S. Smith, C. D. H. Williams, and A. F. G. Wyatt, New J. Phys. **9**, 52 (2007).

<sup>11</sup>M. A. H. Tucker and A. F. G. Wyatt, J. Phys.: Condens. Matter **6**, 2813 (1994).

<sup>12</sup>M. A. H. Tucker and A. F. G. Wyatt, J. Low Temp. Phys. **113**, 621 (1998).

<sup>13</sup>I. N. Adamenko, K. E. Nemchenko, A. V. Zhukov, M. A. H. Tucker, and A. F. G. Wyatt, Phys. Rev. Lett. **82**, 1482 (1999).

<sup>14</sup>R. A. Sherlock, N. G. Mills, and A. F. G. Wyatt, J. Phys. C **8**, 2575 (1975).

<sup>15</sup>W. G. Stirling, *75th Jubilee Conference on Liquid Helium*, 4th ed., edited by J. G. M. Armitage (World Scientific, Singapore, 1983), p. 109.

<sup>16</sup>S. Havlin and M. Luban, Phys. Lett. A **42**, 133 (1972).

<sup>17</sup>M. A. H. Tucker, A. F. G. Wyatt, I. N. Adamenko, A. V. Zhukov, and K. E. Nemchenko, Low Temp. Phys. **25**, 488 (1999) [Fiz. Nizk. Temp. **25**, 657 (1999)].

<sup>18</sup>I. N. Adamenko, Yu. A. Kitsenko, K. E. Nemchenko, V. A. Slipko, and A. F. G. Wyatt, Low Temp. Phys. **31**, 459 (2005) [Fiz. Nizk. Temp. **31**, 607 (2005)].

<sup>19</sup>M. A. H. Tucker and A. F. G. Wyatt, J. Phys.: Condens. Matter **4**, 7745 (1992).

<sup>20</sup>I. N. Adamenko, Yu. A. Kitsenko, K. E. Nemchenko, V. A. Slipko, and A. F. G. Wyatt, Phys. Rev. B **72**, 054507 (2005).

<sup>21</sup>I. N. Adamenko, K. E. Nemchenko, and A. F. G. Wyatt, J. Low Temp. Phys. **125**, 1 (2001).

<sup>22</sup>I. N. Adamenko, Yu. A. Kitsenko, K. E. Nemchenko, V. A. Slipko, and A. F. G. Wyatt, Phys. Rev. B **73**, 134505 (2006).

<sup>23</sup>I. N. Adamenko, Yu. A. Kitsenko, K. E. Nemchenko, V. A. Slipko, and A. F. G. Wyatt, Low Temp. Phys. **33**, 387 (2007) [Fiz. Nizk. Temp. **33**, 523 (2007)].

<sup>24</sup>V. M. Apalkov and M. E. Portnoi, Phys. Rev. B **65**, 125310 (2002).

<sup>25</sup>V. M. Apalkov and M. E. Portnoi, Phys. Rev. B **66**, 121303(R) (2002).

<sup>26</sup>V. B. Berestetskii, E. M. Lifshitz, and L. P. Pitaevskii, *Quantum Electrodynamics* (Butterworth-Heinemann, Oxford, 1982), Vol. 4.

<sup>27</sup>L. D. Landau and E. M. Lifshitz, *Quantum Mechanics: Non-relativistic Theory* (Butterworth-Heinemann, Oxford, 1981), Vol. 3.

<sup>28</sup>R. V. Vovk, C. D. H. Williams, and A. F. G. Wyatt, Phys. Rev. Lett. **91**, 235302 (2003).

<sup>29</sup>D. H. S. Smith, R. Vovk, C. D. H. Williams, and A. F. G. Wyatt, New J. Phys. **8**, 128 (2006).

<sup>30</sup>I. N. Adamenko, K. E. Nemchenko, V. A. Slipko, and A. F. G. Wyatt, Phys. Rev. B **69**, 144525 (2004).

<sup>31</sup>M. A. H. Tucker and A. F. G. Wyatt, Physica B **194-196**, 551 (1994).

<sup>32</sup>D. H. S. Smith and A. F. G. Wyatt, Phys. Rev. B **76**, 224519 (2007).